Simple and general correlation for heat transfer during flow condensation inside plain pipes

Carlos A. Dorao[a,*], Maria Fernandino[a]

[a]*Department of Energy and Process Engineering, Norwegian University of Science and Technology, Norway*

Abstract

This work proposes a new general and simple model to determine the local flow condensation heat transfer coefficient inside plain pipes. The model considers two regimes corresponding to high mass fluxes and/or high thermodynamic qualities and low mass fluxes and/or low thermodynamic qualities. For each region, a new model is suggested which resembles the single-phase heat transfer coefficient model but defining an equivalent Reynolds number in terms of the sum of the superficial liquid and vapour Reynolds numbers. The models consider that the superficial vapour Reynolds number plays a major role in controlling the heat transfer coefficient. The model is able to predict the heat transfer coefficient from channels with a hydraulic diameter of 67 μm up to pipes with a hydraulic diameter of 20 mm for several fluids. No noticeable effect of the diameter of the channel, shape or fluid properties on the heat transfer coefficient has been observed for the studied cases.

Keywords: Flow condensation, Heat transfer coefficient, Two-phase flow

1. Introduction

Condensers based on mini/micro-channels are of great relevance and interest in connection with the growing demand of heat exchangers for several applications ranging from condensers of cooling equipment and air conditioning systems, horizontal tubular evaporators of water-desalinating thermal units, heaters of power systems, heat pipes, etc. Furthermore, in some

*e-mail: carlos.dorao@ntnu.no

applications heat exchangers are the main component in cryogenic processes like separation units and liquefaction of natural gas plants, and the design and performance of the unit can affect some other major equipments like compressors and drivers [1].

During the last decades a large number of models of flow condensation inside pipes has been proposed and tested against experimental data bases as reviewed in the literature by several authors, e.g. [2, 3, 4, 5]. In spite of the extensive work, the general characteristics of the heat transfer phenomena and which are the dominant mechanisms remain an elusive question. This fact is observed in the different dimensionless groups considered in the models suggested under different assumptions. In some cases more than 10 dimensionless groups and adjusted parameters are needed for predicting the experimental data.

The goal of this work is to present a condensation heat transfer coefficient model for flow inside plain pipes. The approach is based on identifying the dominant dimensionless groups and their effect on the heat transfer coefficient of experimental data gathered from the literature. In this work, it will be shown that the heat transfer coefficient shows a distinctive behaviour at high mass fluxes and/or high thermodynamic qualities and low mass fluxes and/or low thermodynamic qualities, fact that is considered for proposing a model for each region.

1.1. Literature review

Extensive reviews of heat transfer models for flow condensation inside pipes can be found in [2, 3, 4, 5]. In this section, the focus will be on highlighting the difference in the selected dimensionless groups considered in some selected models. Table 1 and 2 summarise the models discussed in this section. A common reference for most heat transfer models is the single-phase heat transfer coefficient in pipes. The equation attributed to Dittus-Boelter and McAdams [6], following the equation proposed by Nusselt (1910) based on similarity theory (as cited in [7]), contains only 2 dimensionless groups and 3 adjusted parameters,

$$Nu = \frac{hD}{k} = f_1(Re)f_2(Pr) = CRe^n Pr^m \tag{1}$$

where h is the heat transfer coeficient, D the diameter of the pipe, k the thermal conductivity of the fluid, $Re = GD/\mu$ the Reynolds number (with G the mass flux and μ the dynamic viscosity), $Pr = c_P\mu/k$ the Prandtl number

(with c_p the specific heat). The exponent m is suggested to be 0.3 and 0.4 for cooling and for heating respectively, $n = 0.8$ and the scaling constant $C = 0.023$. The model is based on two functional forms representing the hydrodynamic and thermodynamic effects or influence of the fluid properties $f_1(.)$ and $f_2(.)$ respectively. Several models were suggested later based on larger experimental data bases for example for taking into account the change of the fluid properties with temperature [8, 9], effect neglected in the discussed model, or the shape of the pipe [10].

One of the first correlations available in the literature regarding flow condensation inside pipes was developed by Crosser [11] assuming that the condensate form an annular ring surrounding a turbulent vapour core. The model considers the vapour velocity and the viscosity of the liquid phase for defining an equivalent superficial vapour Reynolds number. Crosser has pointed out to previous research work identifying the direct effect of the vapour velocity on the heat transfer coefficient, namely Jakob, Erk and Eck (1932), Schmidt(1937) and Carpenter and Colburn (1951) (as cited in [11]). The experimental data show good agreement with the model and the exponent n of the equivalent Reynolds number was 0.2 at low Reynolds number approaching 0.8 at high Reynolds number. Rosson [12] developed a model for semi-stratified and laminar annular flow similar to the model of Crosser. The model considers that the heat transfer coefficient is a function of the thickness of the liquid boundary layer that depends on the temperature difference across the liquid film. Akers, Deans and Crosser (1958) (as cited in [12]) proposed a model based on the idea that the vapour core might be replaced with a liquid flow that produces the same liquid-vapour interfacial shear stress. An equivalent Reynolds number was defined and then replaced in the single phase Sieder-Tate (1937) equation [13]. The local condensation heat transfer coefficient is given as

$$Nu = \frac{hD}{k_L} = CPr_L^m \; Re_{eq}^n \tag{2}$$

with the equivalent Reynolds number defined as

$$Re_{eq} = G\left[(1-x) + x\left(\frac{\rho_L}{\rho_V}\right)^{0.5}\right]\frac{D}{\mu_L} \tag{3}$$

with G the mass flux, x the thermodynamic quality, and ρ_L and ρ_V the liquid and vapour density respectively. The model contains 3 adjusted parameters,

$m = 1/3$ and $C = 0.026$ and $n = 0.8$ for $Re_{eq} > 50000$, and $C = 5.03$ and $n = 1/3$ for $Re_{eq} < 50000$.

The influence of the vapour flow rate has also been acknowledged by Goodykoontz and Dorsch [14, 15] who studied condensation of steam in vertical tubes. The experimental data was correlated in terms of the product of the quality and the square of the total mass flux, although, a general model was not provided.

Cavallini and Zecchin (1974) [16] proposed a similar model to the one from Akers, Deans and Crosser (1958) but considering another value for the scaling constant C probably as a consequence of the different fluids studied. The model was suggested for dominant annular flow regime.

It is possible to see that the first available models were considering a direct influence of the vapour flow rate on the heat transfer coefficient. This influence observed in the experiments was implemented in the models by including the product of the total mass flux and the quality, i.e. $G\ x$. Later models have considered alternative descriptions and the dependency on the vapour velocity was introduced in an indirect manner in some cases by multipliers applied to a single phase Dittus-Boelter heat transfer model.

Shah (1979) [17] suggested a dimensionless correlation for predicting heat transfer coefficient during film condensation inside pipes by considering the similarity between the mechanisms of film condensation and boiling without bubble nucleation. The model results in an expression containing 9 adjustable parameters and 5 dimensionless groups. The reduced pressure $P_R = P/P_C$ was introduced in the model while the dependency on the liquid-vapour density ratio was removed compared with the previous two discussed models. The model was extended to two regimes in [18]. The regime transition is defined in terms of the dimensionless vapour velocity, J_G, and Shah's correlating parameter, Z, given as

$$J_G^T = \frac{1}{2.4Z + 0.263} \text{ with } Z = \left(\frac{1}{x} - 1\right)^{0.8} P_R^{0.4} \tag{4}$$

and

$$J_G = \frac{Gx}{(g\ D\ \rho_g(\rho_l - \rho_g))^{0.5}} \tag{5}$$

Tandon et al. (1995) [19] proposed a modification to the Akers, Deans and Crosser (1958) correlations based on condensation experiments for R12 and R22 acknowledging the direct dependency of the heat transfer coefficient

on the average vapour mass velocity. It is considered that a high vapour mass velocity results in a higher turbulence of the liquid film increasing the heat transfer coefficient. They also observed a change in slope in the heat transfer coefficient versus the equivalent vapour Reynolds number defined in terms of the liquid viscosity, i.e. [11]. The change in the slope is attributed to changes from annular and semi-annular flow to wavy flow. The model introduced the Jakob number defined as $(h_{LV}/C_P\Delta T)$ where ΔT is the temperature difference across the condensate film. The model is presented with two branches where the exponent changes from $n = 0.67$ to $n = 0.125$ from the defined shear-controlled flow (annular and semi-annular) to the gravity-controlled flow (wavy flow).

Dobson and Chato (1998) [20] suggested a model considering an annular flow and a wavy flow regime. For the annular flow regime, the model is similar to the single-phase flow heat transfer coefficient equation but multiplied by a term including the Martinelli parameter X_{tt}. For the wavy flow regime, the model considers a separate heat transfer contribution by the film condensation in the upper part of the horizontal tube from the forced-convective heat transfer in the bottom pool. The model for film condensation includes the liquid Jacob and the Galileo number. The boundary for the transition from the annular to the wavy flow region is given in term of $G > 500 kg/m^2 s$ or $Fr_{so} < 20$, where Fr_{so} is the Soliman's modified Froude number

$$Fr_{so} = 0.025 Re_L^{1.59} \left(\frac{1 + 1.09 X_{tt}^{0.039}}{X_{tt}} \right)^{1.5} \frac{1}{Ga^{0.5}} \quad \text{for } Re_L \leq 1250 \qquad (6)$$

$$Fr_{so} = 1.26 Re_L^{1.04} \left(\frac{1 + 1.09 X_{tt}^{0.039}}{X_{tt}} \right)^{1.5} \frac{1}{Ga^{0.5}} \quad \text{for } Re_L > 1250 \qquad (7)$$

The final model for the wavy regime include 7 dimensionless groups and more than 10 adjusted coefficients.

Cavallini et al. (2006) [21] suggested a model considering a ΔT-dependent and a ΔT-independent flow regimes, where ΔT is referred to the temperature difference between the wall and the fluid temperature. The model for the ΔT-independent flow regime was based on correcting the liquid phase heat transfer coefficient by a two-phase multiplier containing the liquid-vapour density ratio, liquid-vapour viscosity ratio and the liquid Pr number resulting in 7 dimensionless groups and 9 adjusted parameters. The model for

the ΔT-dependent regime is constructed considering the model for the ΔT-independent regime and a model that includes the a progressive transition from wavy-stratified to the smooth stratified flow. The transition boundary for the two regions is given as

$$J_G^T = \left[\left(\frac{7.5}{4.3 X_{tt}^{1.111} + 1} \right)^{-3} + C_T^{-3} \right]^{-1/3} \tag{8}$$

where C_T is 1.6 for hydrocarbons and 2.6 for other refrigerants.

Recently, Dorao and Fernandino [22] studied the heat transfer coefficient during flow condensation inside plain pipes. By studying the dependency of the local heat transfer coefficient in terms of dimensionless groups, it was possible to identify that the sum of the superficial liquid and vapour Reynolds number alone can describe the heat transfer process for high mass fluxes. Although it has been acknowledged in the literature that the magnitude of the shear between the liquid and vapour results in diverse interfacial phenomena that might influence the heat transfer coefficient, the explicit consideration of the sum of the superficial liquid and vapour Reynolds number on the heat transfer coefficient has not been considered in previous models. However, in previous experimental studies of non-boiling two-components two-phase flows, e.g. air-water, the heat transfer coefficient has been correlated by the sum of the liquid and gas Reynolds number [23, 24]. The model suggested by Dorao and Fernandino reflects also the direct effect of the vapour velocity on the heat transfer coefficient observed in previous work. The model is identical to the Dittus-Boelter model but in terms of an equivalent two phase flow Reynolds and Prandtl number and containing only 3 adjusted parameters equals to the ones from the Dittus-Boelter correlations which gives a correct transition to the single phase heat transfer coefficient model.

In summary, several models are available in the literature for predicting flow condensation heat transfer coefficient inside plain pipes. However, there is no common agreement about which dimensionless groups should be considered in the models which is a consequence that the dominant mechanisms controlling heat transfer have not been properly identified. Nevertheless it is possible to observe that most of the models share a similar structure to the single-phase flow heat transfer coefficient equation multiplied by a function of diverse dimensionless groups. In general, the heat transfer coefficient models consider two regions related to high mass fluxes or dominant annular flow regime and to low mass fluxes or wavy or/and stratified flow regime. In

Author(s)	Equation
Crosser (1955) [11]	$Nu = CPr_L^{1/3}\left\{G\left[x\left(\frac{\rho_L}{\rho_V}\right)^{0.5}\right]\frac{D}{\mu_L})\right\}^n$ $C = 0.0265\ n = 0.8$ for $\frac{Gx}{\mu_L} > 60000$ $n = 0.2$ for $\frac{Gx}{\mu_L} < 60000$
Rosson (1957) [12]	$Nu = CPr_L^{1/3}\left[\frac{g\rho_L - \rho)\rho_L h_{lv} R}{12k_L\mu_L\Delta T}\right]^{0.6}\left\{G\left[x\left(\frac{\rho_L}{\rho_V}\right)^{0.5}\right]\frac{D}{\mu_L})\right\}^n$ $C = 0.388\ n = 0.25$ for $\frac{GxD}{\mu_L}\left(\frac{\rho_L}{\rho_V}\right)^{0.5} < 60000$
Akers et al. (1958)	$Nu = CPr_L^{1/3}\left\{G\left[(1-x) + x\left(\frac{\rho_L}{\rho_V}\right)^{0.5}\right]\frac{D}{\mu_L})\right\}^n$ $C = 0.026\ n = 0.8$ for $Re_{eq} > 50000$ $C = 5.3\ n = 1/3$ for $Re_{eq} < 50000$
Goodykoontz and Dorsch (1967) [14, 15]	$Nu \propto G^2 x$
Cavallini and Zecchin (1974) [16]	$Nu = 0.05Re_L^{0.8}Pr_L^{0.33}\left[1 + \frac{x}{(1-x)}\left(\frac{\rho_L}{\rho_V}\right)^{0.5}\right]^{0.8}$
Shah (1979) [17]	$Nu = 0.023Re_{L0}^{0.8}Pr_L^{0.4}\left[(1-x)^{0.8} + \frac{3.8x^{0.76}(1-x)^{0.04}}{P_R^{0.38}}\right]\frac{D}{k_L}$
Shah (2009) [18]	$Nu = Nu_I \qquad J_G \geq 0.98\left((1/x-1)^{0.8}P_R^{0.4} + 0.263\right)^{-0.62}$ $Nu = Nu_I + Nu_{Nu} \qquad J_G < 0.98\left((1/x-1)^{0.8}P_R^{0.4} + 0.263\right)^{-0.62}$ $Nu_I = 0.023Re_{L0}^{0.8}Pr_L^{0.4}(\frac{\mu_L}{14\mu_V})^n\left[(1-x)^{0.8} + \frac{3.8x^{0.76}(1-x)^{0.04}}{P_R^{0.38}}\right]$ $n = 0.0058 + 0.557P_R$ $Nu_{Nu} = 1.32Re_{L0}^{-1/3}\left[\frac{\rho_L(\rho_L - \rho_V)g\ k_L^3}{\mu_L^2}\right]^{1/3}$

Table 1: Some previous flow condensation heat transfer correlations

the next sections, the model for high mass fluxes presented in [22] will be the introduced, then the influence of the low mass fluxes and/or low thermodynamic qualities is discussed that will result in a new model for this region.

Author(s)	Equation
Tandon et al. (1995) [19]	$Nu = CPr_L^{1/3}\left(\frac{h_{LV}}{C_p\Delta T}\right)\left(Re_V^*\right)^n$
	$C = 0.084$ $n = 0.67$ for $Re_V^* = \frac{Gx}{\mu_L} > 30000$
	$C = 23.1$ $n = 1/8$ for $Re_V^* < 30000$
Dobson and Chato (1998) [20]	$Nu = Nu_a$ if $G > 500kg/m^2s$ or $Fr_{so} < 20$
	$Nu = Nu_w$ if $G < 500kg/m^2s$ or $Fr_{so} > 20$
	$Nu_a = 0.023Re_L^{0.8}Pr_L^{0.4}\left(1 + \frac{2.22}{X_{tt}^{0.89}}\right)$
	$Nu_w = \frac{0.23Re_{V0}^{0.12}}{1 + 1.11X_{tt}^{0.58}}\left[\frac{GaPr_L}{Ja_L}\right]^{0.25} +$
	$\times(1 - \theta_L/\pi)0.0195Re_L^{0.8}Pr_L^{0.4}\left(1.376 + \frac{c_1}{X_{tt}^{c_2}}\right)^{0.5}$
	$c_1 = 4.172 + 5.48Fr_L - 1.564Fr_L^2$ $0 < Fr \leq 0.7$
	$c_1 = 7.242$ $Fr > 0.7$
	$c_2 = 1.773 - 1.655Fr_L$ $0 < Fr \leq 0.7$
	$c_2 = 1.655$ $Fr > 0.7$
	$\alpha = \frac{\theta_L}{\pi} - \frac{sin(2\theta_L)}{2\pi}$
Cavallini et al. (2006) [21]	$h = h_A$ if $J_G > J_G^T$
	$h = h_D$ if $J_G \leq J_G^T$
	$h_A = 0.023Pr_L^{0.4}Re_{L0}^{0.8}\left[1 + 1.128x^{0.8170}\right.$
	$\times\left(\frac{\rho_L}{\rho_G}\right)^{0.3685}\left(\frac{\mu_L}{\mu_G}\right)^{0.2363}\left(1 - \frac{\mu_G}{\mu_L}\right)^{2.144}Pr_L^{-0.1}\left.\right]$
	$h_D = \left[h_A(\frac{J_G^T}{J_G})^{0.8} - h_S\right](\frac{J_G}{J_G^T}) + h_S$
	$h_S = 0.725\left[1 + 0.741\left(\frac{1-x}{x}\right)^{0.3321}\right]^{-1}$
	$\times\left[\frac{k_L^3\rho_L(\rho_L - \rho_V)gh_{LV}}{\mu_L D\Delta T}\right]^{0.25} + (1 - x^{0.0087})0.023Pr_L^{0.4}\ Re_{L0}^{0.8}\frac{k_L}{D}$
Dorao and Fernandino (2017) [22]	$Nu = 0.023(Re_V + Re_L)^{0.8}(Pr_L(1-x) + Pr_V x)^{0.3}$
	$G \geq 200kg/m^2s$ and $0 < x < 1$
This work	$Nu_= \left[Nu_I^9 + Nu_{II}^9\right]^{1/9}$
	$Nu_I = 0.023(Re_V + Re_L)^{0.8}(Pr_L(1-x) + Pr_V\ x)^{0.3}$
	$Nu_{II} = (41.5D^{0.6})(Re_V + Re_L)^{0.4}(Pr_L(1-x) + Pr_V\ x)^{0.3}$
	$for 0 < x < 1$ and $67\mu m < D_h < 20mm$

Table 2: Cont. Table 1. Some previous flow condensation heat transfer correlations

2. Method

In this study, experimental data from the literature has been gathered covering a large range of fluids and pipe diameters. The experimental data considered is summarised in Table 3. The fluid properties are calculated with the software REFPROP version 9.1 [25] at the saturation conditions of the fluid. The largest individual data set (i.e. for a given fluid and pipe diameter) represents only the 8% of the total number of experimental data points. Figure (1) shows the distribution of the data point in terms of the reduced pressure P_R and pipe diameter.

In the next section the accuracy of the models is evaluated by $\theta_{\pm 10\%}$, $\theta_{\pm 20\%}$

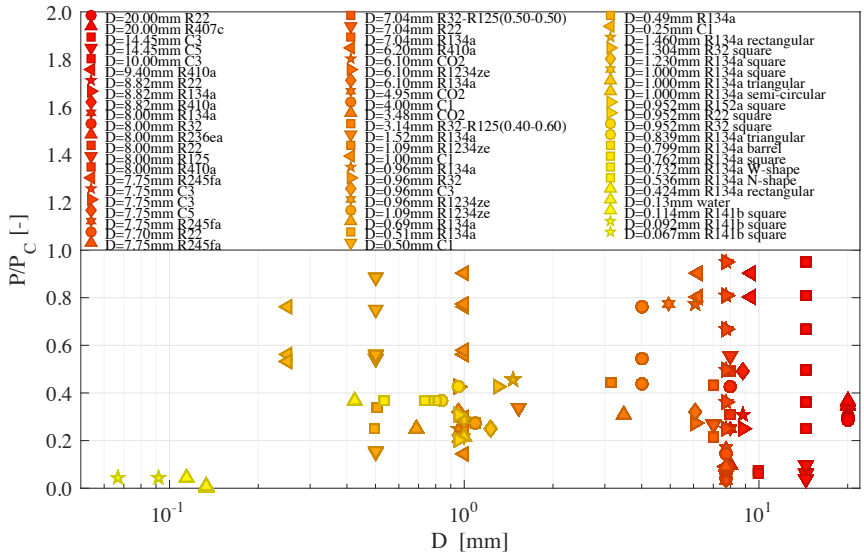

Figure 1: Distributions of number of data point in terms of reduced pressure, P_R, and pipe diameter, D.

and $\theta_{\pm 30\%}$, the percentage of data points predicted within $\pm 10\%$, $\pm 20\%$ and $\pm 30\%$ respectively, and the average and mean absolute error, defined as

$$AVG = \frac{1}{N} \sum \frac{Nu_{pred} - Nu_{exp}}{Nu_{exp}} \times 100 \tag{9}$$

$$MAE = \frac{1}{N} \sum \frac{|Nu_{pred} - Nu_{exp}|}{Nu_{exp}} \times 100 \tag{10}$$

Author(s)	Fluid	Diameter [mm]	shape	G [kg/m^{-2} s]	T_{sat} [$^{\circ}C$]	Points
Aprea et al. (2003) [26]	R22	20.00	circular	45.5-120	37.1-39.6	65
	R407c	20.00	circular	47-115	36.6-38.8	55
McDonald (2015) [27]	C3	14.45	circular	150-450	30-94	151
Milkie (2014) [28]	C5	14.45	circular	100-450	45-75	98
Yu et al. (2017)* [29]	C3	10.00	circular	224-394	-19–13.7	46
Mitra (2005) [30]	R410a	9.40	circular	200-800	61.1-66.6	236
Jung et al.(2004)[31]	R22	8.82	circular	100-300	40	36
	R134a	8.82	circular	100-300	40	27
	R410a	8.82	circular	100-300	40	26
Cavallini et al.(2001) [32]	R134a	8.00	circular	65-750	40	49
	R32	8.00	circular	100-600	40	22
	R236ea	8.00	circular	100-600	40	33
	R22	8.00	circular	100-750	40	82
	R125	8.00	circular	100-750	40	21
	R410a	8.00	circular	100-750	40	41
McDonald (2015) [27]	C3	7.75	circular	150-450	30-94	135
Ghim et al. (2017) [33]	R245fa	7.75	circular	150-700	50	21
Milkie (2014) [28]	C5	7.75	circular	150-600	45-60	74
	R245fa	7.75	circular	150-600	20-70	93
Shin et al.(1997) [34]	R22	7.70	circular	424-743	12	25
Dobson et al.(1998) [20]	R32-R125(0.50-0.50)	7.04	circular	75-650	35	21
	R22	7.04	circular	75-650	35	27
	R134a	7.04	circular	75-650	35	19
Mitra (2005) [30]	R410a	6.20	circular	200-800	61.1-66.6	221
Kondou et al. (2011) [35]	CO2	6.10	circular	100-200	20-20	47
Agarwal et al. (2015) [36]	R1234ze	6.10	circular	100-300	50	37
Xiao et al. (2016) [37]	R134a	6.10	circular	50-200	50	45
Son (2012) [38]	CO2	4.95	circular	400-800	20	18
Xiao et al. (2017) [39]	C1	4.00	circular	99-255	-107–91	231
Kim et al. (2008) [40]	CO2	3.48	circular	200-800	-15	16
Dobson et al.(1998) [20]	R32-R125(0.40-0.60)	3.14	circular	75-800	35	46
Bandhauer et al(2006) [41]	R134a	1.52	circular	150-750	52	58
Liu et al.(2016) [42]	R1234ze	1.09	circular	200-800	50	14
Maraak (2009) [43]	C1	1.00	circular	160-700	-132.3–85.7	105
Matkovic(2009) [44]	R134a	0.96	circular	100-1200	40	87
	R32	0.96	circular	100-1200	40	73
Del Col et al.(2012) [45]	C3	0.96	circular	100-800	40	53
Del Col et al.(2015) [46]	R1234ze	0.96	circular	200-800	40	27
Liu et al.(2016) [42]	R1234ze	1.09	circular	200-800	50	14
Shin et al.(2005)[47]	R134a	0.69	circular	400-600	40	36
Bandhauer et al.(2006) [41]	R134a	0.51	circular	450-750	52	23
Maraak (2009) [43]	C1	0.50	circular	275-1360	-131.4- -86.3	48
Shin et al.(2005) [47]	R134a	0.49	circular	200-600	40	27
Maraak (2009) [43]	C1	0.25	circular	1140-1225	-101.7- -91	14
Wang et al.(2002) [48]	R134a	1.460	rectangular	250-750	64	299
Liu et al.(2015) [49]	R32	1.304	square	200-600	40	24
Del Col et al.(2011)[50]	R134a	1.230	square	392-789	40	219
Derby et al. (2012)[51]	R134a	1.000	square	150-450	35-45	113
	R134a	1.000	triangular	150-450	35	59
	R134a	1.000	semi-circular	150-450	35	42
Liu (2015) [49]	R152a	0.952	square	400-600	40	18
	R22	0.952	square	400-600	40	15
	R32	0.952	square	200-600	40	24
Agarwal (2010) [52]	R134a	0.839	triangular	300-750	55	31
	R134a	0.799	barrel	300-750	55	28
	R134a	0.762	square	300-750	55	35
	R134a	0.732	W-shape	300-750	55	29
	R134a	0.536	N-shape	300-750	55	24
	R134a	0.424	rectangular	450-750	55	11
Zhang et al. (2013) [53]	water	0.133	square	200-300	103-115	261
Dong et al. (2008)[54]	R141b	0.114	square	200	51	14
	R141b	0.092	square	200	51	13
	R141b	0.067	square	200	51	12
Total						3937

* Helical tube

Table 3: Condensation heat transfer database for mini/micro-channel flows.

2.1. Heat transfer coefficient at high mass fluxes, Nu_I

A new model for the heat transfer coefficient inside tubes for high mass fluxes ($G > 200 kg/m^2 s$), Nu_I, has been developed in [22]. The model is given as

$$Nu_I = 0.023 Re_{2\phi}^{0.8} Pr_{2\phi}^{0.3} \tag{11}$$

with

$$Re_{2\phi} = Re_L + Re_V = \frac{GxD}{\mu_V} + \frac{G(1-x)D}{\mu_L} \quad \text{for } 0 < x < 1 \tag{12}$$

a two-phase flow equivalent Reynolds number defined in terms of the sum of the superficial vapour and liquid Reynolds number, and

$$Pr_{2\phi} = Pr_L(1-x) + Pr_V\ x \quad \text{for } 0 < x < 1 \tag{13}$$

an equivalent two-phase flow Prandtl number. The coefficients in the model correspond to the ones from the correlation of Dittus-Boelter for the single phase flow heat transfer coefficient. In this way, the model approaches the all liquid and all vapour single phase flow heat transfer coefficient as the quality approaches 0 and 1 respectively.

The prediction capability of the new model is shown in Figure (2) against the experimental data base of 3006 experimental data points with mass fluxes $G \geq 200 kg/m^2$s. The new model predicts 86.4% of the Nusselt number to within ±30%. Some data points show some deviation (methane in a 0.25mm diameter pipe [43], propane in a 7.75 mm diameter pipe at high saturation temperature [27]) but authors have acknowledged the high uncertainty of the data points due to the challenging conditions of the experiments. It is noted that no influence of the pipe diameter is observed for the experimental data points ranging from 67 μm to 14.45 mm. The similitude of the proposed model to the single phase heat transfer coefficient model might indicate that similar heat transfer mechanisms are dominant in both situations. Experimental and numerical studies of heat transfer in single phase flow inside pipes [55, 56, 57] have shown that the thermal resistance is mainly concentrated in the conductive sublayer and beyond this sublayer a rapid diffusion of the heat into the bulk flow is observed. This assumption was tested in [22, 58] by considering flow condensation inside micro-channels of different shapes, flow condensation of binary mixtures, flow boiling at low heat fluxes, i.e. avoiding bubble nucleation, and non-boiling two phase flows for slug and annular flow regimes. As the suggested model was able to capture the trend of such cases, it is possible to consider that the heat transfer might be controlled at the

conductive sublayer and events occurring far from this sublayer, i.e. different flow patterns, do not have major influence on the heat transfer coefficient. In particular, no effect of the diameter of the channel on the heat transfer coefficient has been observed. This fact can be attributed to the fact that the slope of the variation of the single phase Nusselt number with Reynolds number at high Reynolds number is consistent with the predicted slope from the Dittus-Boelter model [59].

The relationship between the single phase flow heat transfer coefficient and the heat transfer coefficient for flow condensation based on the Dittus-Boelter model should also be valid for other single phase models. As an example, the model of Petukhov & Krillov (1958), cited by [10],

$$Nu = \frac{f/8RePr}{k_1 + 12.7(f/8)^{0.5}(Pr_L^{2/3} - 1)} \tag{14}$$

$$k_1 = 1.07 + \frac{900}{Re} - \frac{0.63}{1 + 10Pr} \tag{15}$$

$$f = (0.79ln(Re) - 1.64)^{-2} \tag{16}$$

for fully developed flow is considered where the single phase Reynolds and Prandtl numbers are replaced for $Re_{2\phi}$ and $Pr_{2\phi}$, respectively. Figure (3) shows the error in terms of Nu_{cal}/Nu_{exp} versus the thermodynamic quality of experimental data points with $G \geq 200kg/m^2s$. The model predicts 75.2% of the Nusselt number to within ±30% similar to the result shown in figure (2) based on the Dittus-Boelter model.

The previous result might indicate that for enhanced surfaces the heat transfer coefficient during flow condensation is related to the single phase heat transfer coefficient on the surface. Figure (4) shows experimental data corresponding to flow condensation of R1234yf inside a 3.4mm ID microfin pipe [60]. It is possible to see that the flow condensation heat transfer coefficient follows the trend of the single phase heat transfer coefficient for equivalent Reynolds numbers. At high Reynolds number it is expected that heat transfer coefficient approaches the corresponding to the smooth case [61]. However no experimental data set was found presenting experimental heat transfer coefficient measurements for single phase and flow condensation on equivalent Reynolds numbers. The figure also includes a comparison of flow condensation of R22 inside a 4.6mm ID micro-fin pipe [62] where a similar trend is observed. This fact implies that the derived model for the

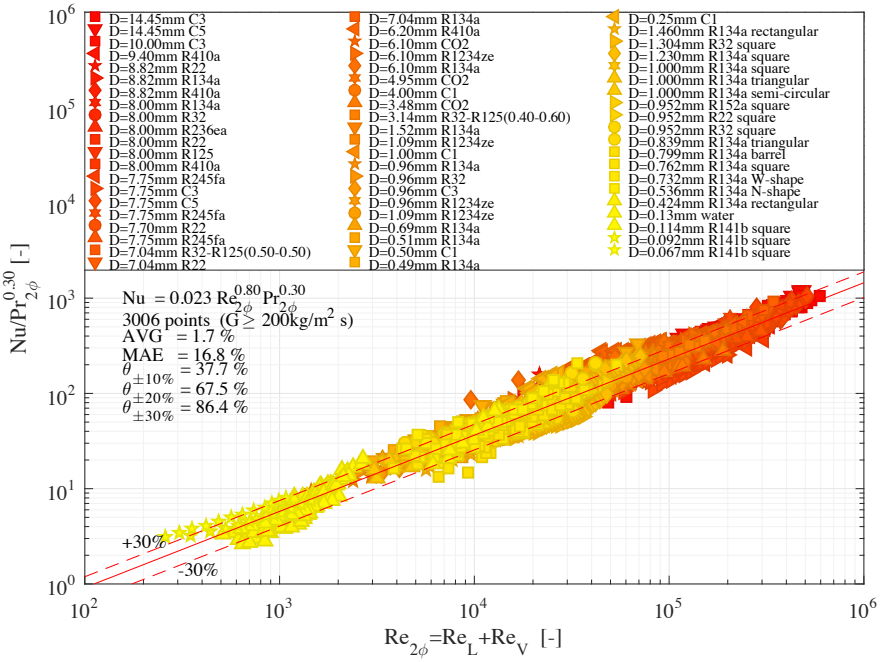

Figure 2: Dependency of $Nu/Pr_{2\phi}^{0.3}$ in terms of $Re_{2\phi}$ for experimental data points with mass fluxes $G \geq 200 kg/m^2 s$.

single phase heat transfer coefficient can be applicable for predicting the flow condensation heat transfer coefficient in enhanced surfaces.

2.2. Heat transfer coefficient at low mass fluxes, Nu_{II}

The goal of this work is to extend the previous model to cases of low mass fluxes. Figure (5) shows experimental data points for a pipe diameter of 8 mm for 6 different refrigerants and mass fluxes from 65 to 750 kg/m^2 s [32] in terms of the $Nu/Pr_{2\phi}^{0.30}$ versus $Re_{2\phi}$. The experimental data shows a departure from the $Re_{2\phi}^{0.8}$ curve almost at the same value of $Re_{2\phi}$ (that will be referred to as $Re_{2\phi,T}$) independent of the working fluid. This departure can be interpreted as an enhancement of the heat transfer. At low qualities and high mass fluxes, bubbles can improve the mixing and thus the heat transfer, while at low mass fluxes, corresponding to stratified flow regime, film condensation in the upper part of the pipe and/or the waves in the film might enhance the heat transfer. At the same time, experiments in this region

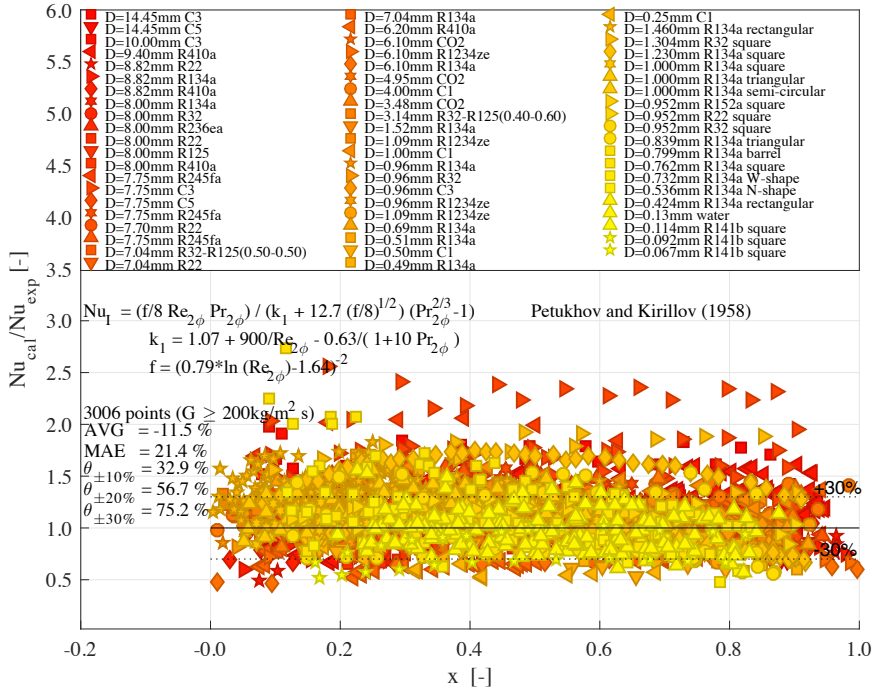

Figure 3: Evaluation of the new model in terms of the thermodynamic quality corresponding to model Nu_I considering the single phase heat transfer coefficient model of Petukhov & Krillov (1958).

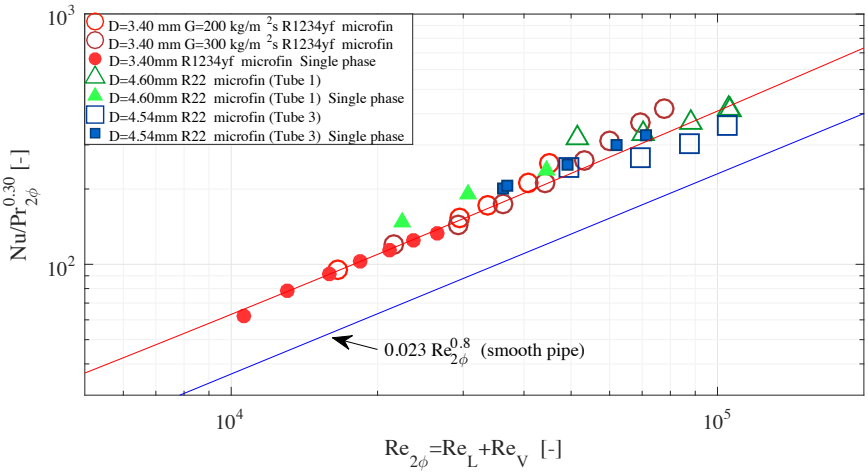

Figure 4: Dependency of $Nu/Pr_{2\phi}^{0.3}$ in terms of $Re_{2\phi}$ for flow condensation of R1234yf inside a 3.4mm ID microfin pipe [60], and flow condensation of R22 inside a 4.6mm ID microfin pipe [62]. For liquid single phase $Re_{2\phi} = Re_{L0}$ and $Pr_{2\phi} = Pr_{L0}$.

can be affected by larger uncertainties e.g. due to the segregation of the flow. However, the experimental data does not shown a clear distinction between these two possible effects and due to the limited number of experimental data points in this region no further analysis was possible. Nevertheless, it is possible to see that the experimental data follows a different curve called Nu_{II} which is expected to depend on the pipe diameter and needs to be determined.

Figure (6) shows the effect of the pipe diameter in the transition value of $Re_{2\phi,T}$ for two different pipe diameter of 8mm [32] and 1.52mm [41]. Considering the dependency of $Re_{2\phi,T}$ for different pipe diameters, the following expression was obtained

$$Re_{2\phi,T} = 10^8 \; D^{1.5} \quad \text{with } D[m] \text{ the pipe diameter} \tag{17}$$

For testing the validity of this model, the experimental data can be ploted in terms of the ratio $[Nu/Pr_{2\phi}^{0.30}]/[Nu/Pr_{2\phi}^{0.30}]_T$ versus the ratio $Re_{2\phi}/Re_{2\phi,T}$, where $[Nu/Pr_{2\phi}^{0.30}]_T$ is computed with Eq. (11) at $Re_{2\phi,T}$, Figure (7). The experimental data points are well captured independent of the fluid and pipe diameter for both regions i.e. Nu_I for $Re_{2\phi}/Re_{2\phi,T} < 1$ and Nu_{II} for $Re_{2\phi}/Re_{2\phi,T} > 1$.

The new general local heat transfer coefficient model for flow condensation

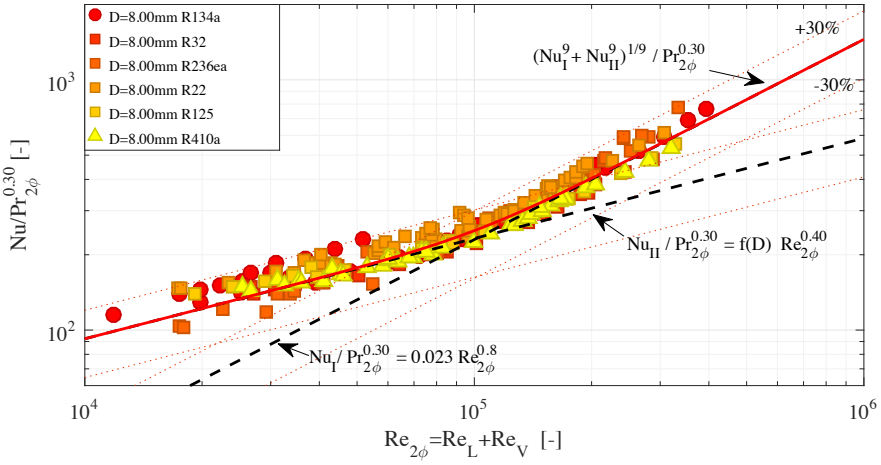

Figure 5: Departure from the Nu_I curve for experimental data at low mass fluxes and low qualities.

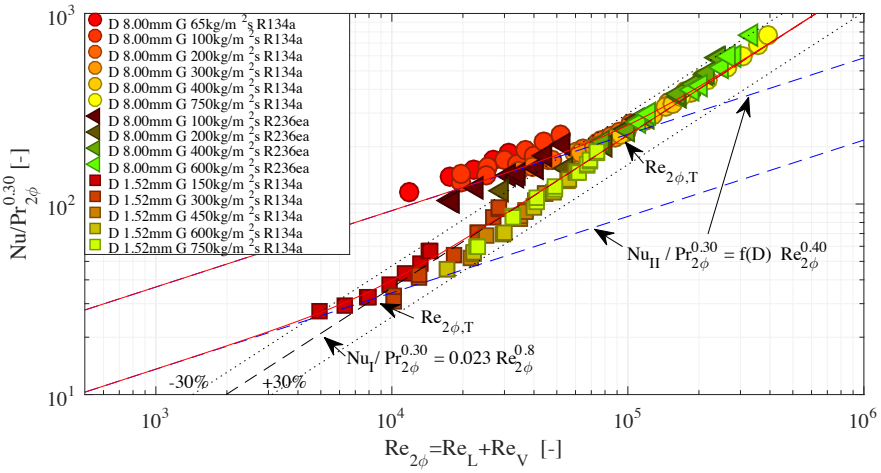

Figure 6: Departure from the Nu_I curve for experimental data at low mass fluxes and low qualities for two different pipe diamters.

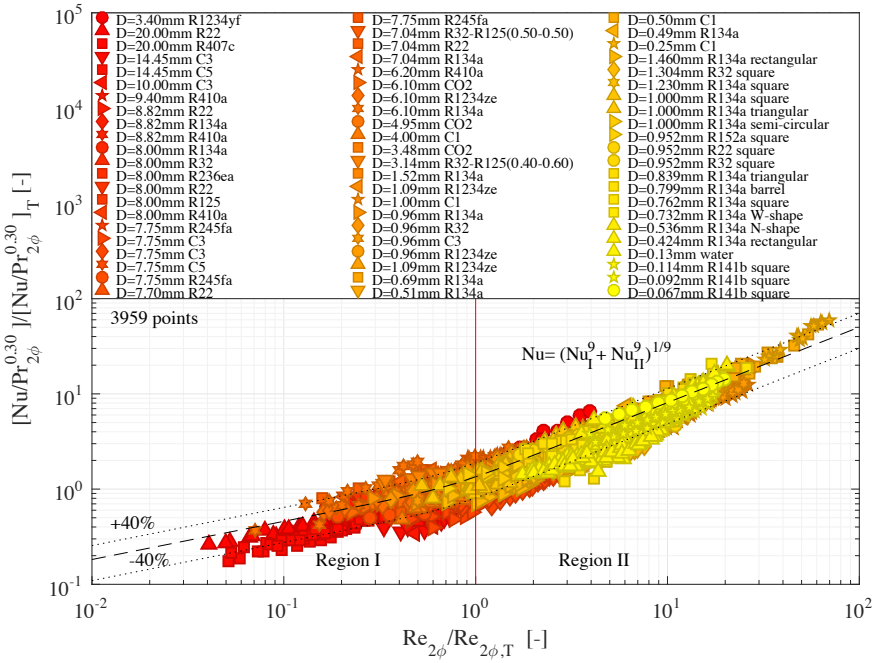

Figure 7: Experimental data points in terms of $Re_{2\phi}/Re_{2\phi,T}$ for evaluating the model of $Re_{2\phi,T}$.

inside plain tubes is given as

$$Nu_I = 0.023 Re_{2\phi}^{0.80} Pr_{2\phi}^{0.30} \quad Re_{2\phi} > Re_{2\phi,T} \tag{18}$$

$$Nu_{II} = 41.5 D^{0.60} Re_{2\phi}^{0.40} Pr_{2\phi}^{0.30} \quad Re_{2\phi} < Re_{2\phi,T} \tag{19}$$

For simplicity, both models can be interpolated [63], with the following expression

$$Nu = \left(Nu_I^9 + Nu_{II}^9 \right)^{1/9} \tag{20}$$

which is shown in Figure 5. The exponent 9 was selected for providing a sharp transition between the models.

Figure (8), (9) and (10) show the deviation of the new model in terms of the thermodynamic quality for the Eq.(18), Eq.(19) and Eq.(20) respectively. The models provide a good agreement with the data for both low and high qualities values. It is observed that experimental points related to propane at high pressure in 7.75 mm diameter pipes show a large deviation as mentioned before. The distribution of the errors corresponding to the previous plots are shown in a histogram in Figure (11). The data points for $Re_{2\phi} < Re_{2\phi,T}$, i.e. region II, shows a larger standard deviation from the mean, but these points are also characterised by larger uncertainties.

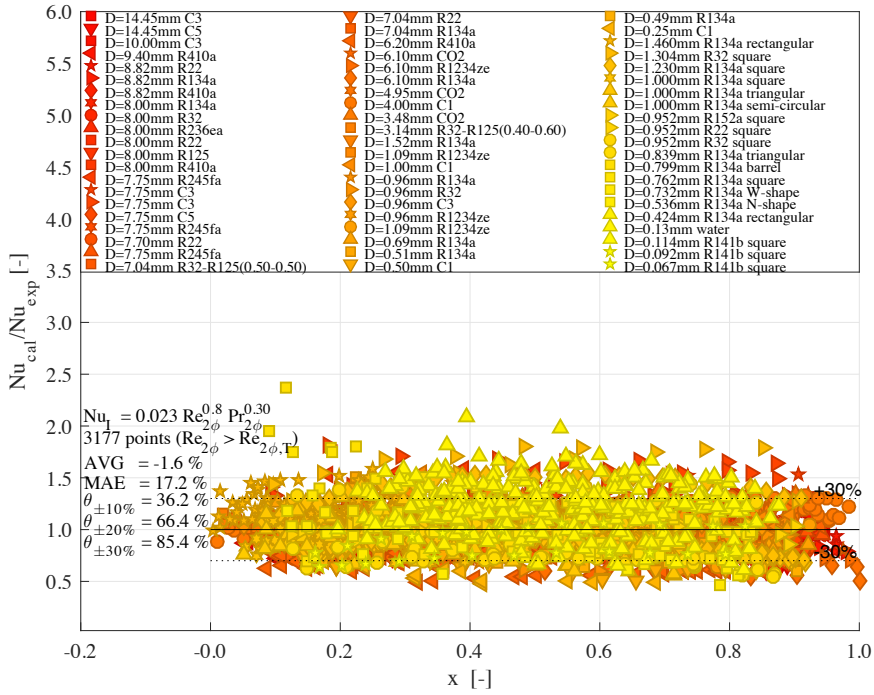

Figure 8: Evaluation of the new model in terms of the thermodynamic quality corresponding to model Nu_I.

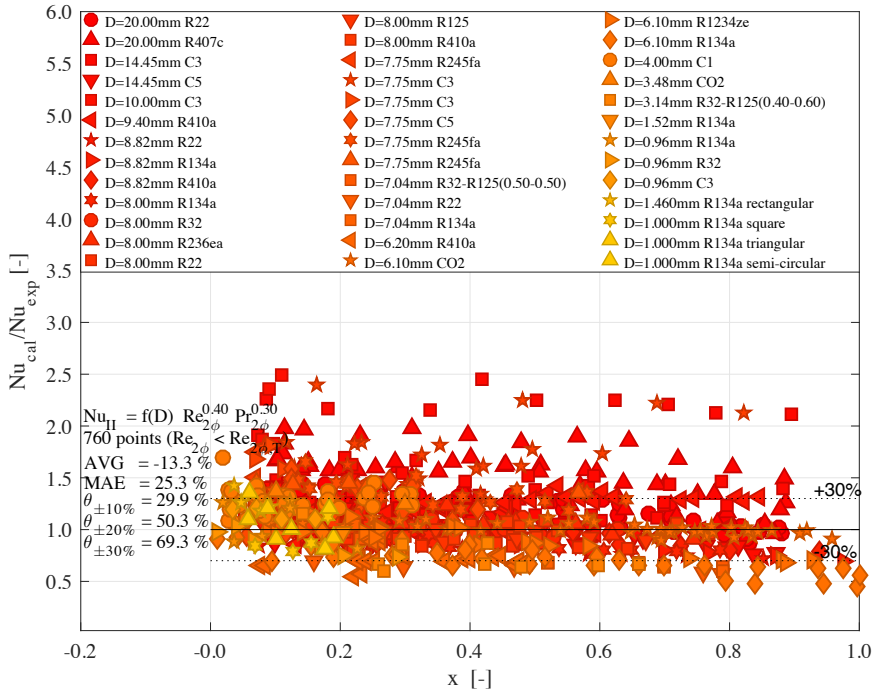

Figure 9: Evaluation of the new model in terms of the thermodynamic quality corresponding to model Nu_{II}.

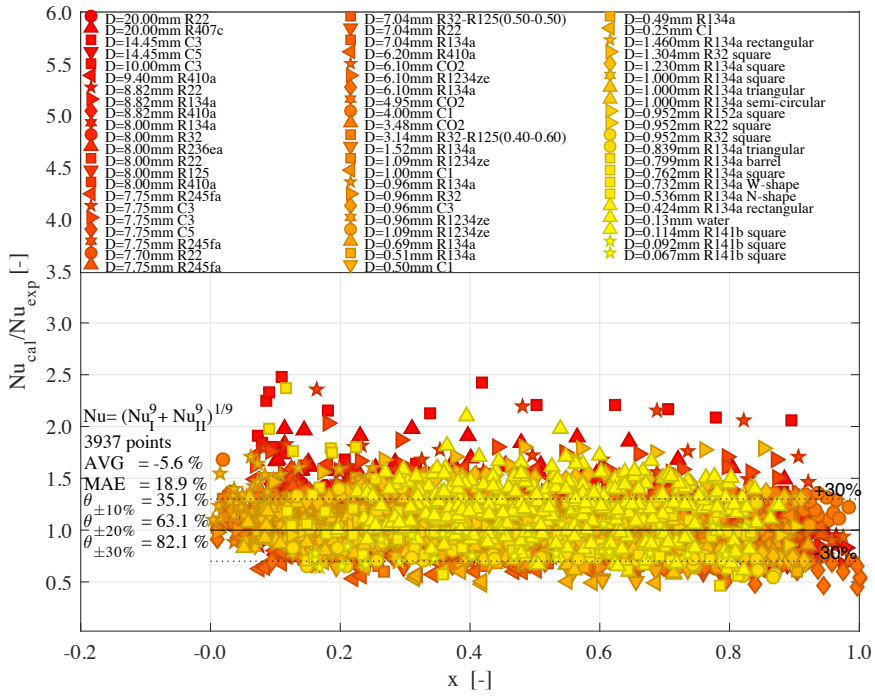

Figure 10: Evaluation of the new model in terms of the thermodynamic quality for model Nu.

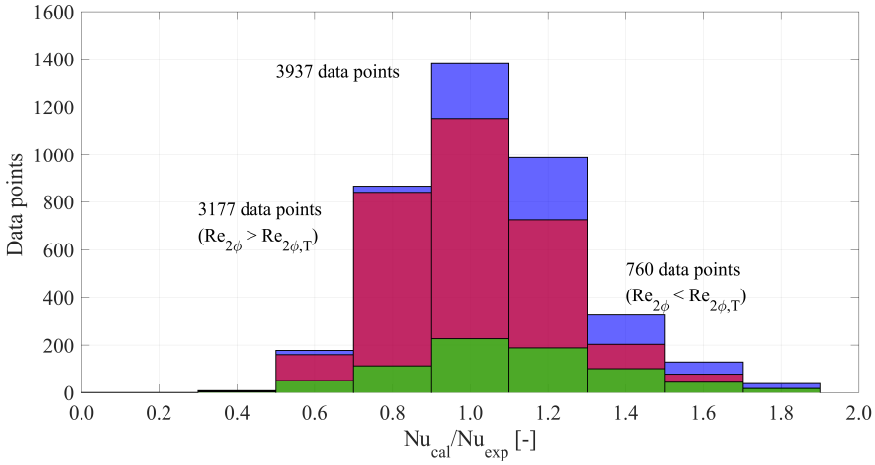

Figure 11: Histogram of the error corresponding to Figure (8), (9) and (10)

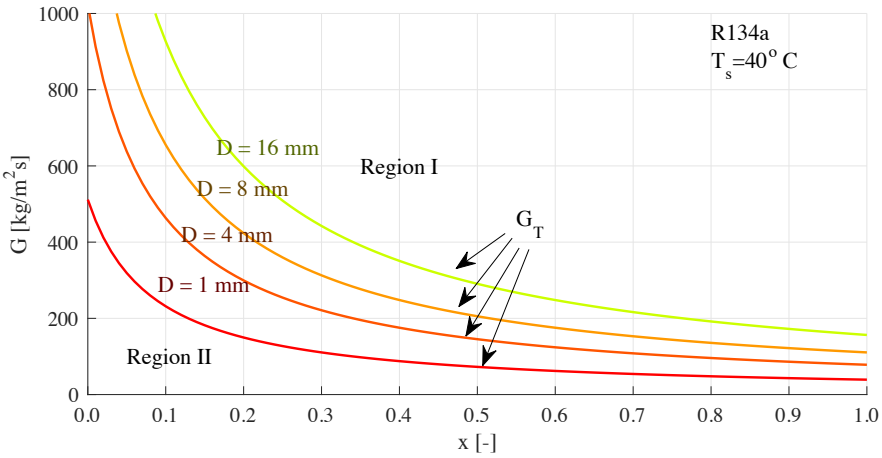

Figure 12: Effect of the pipe diameter in G_T for R134a.

2.3. Effect of the pipe diameter on the transition boundary

The new model suggested in the previous section considers two regions determined by $Re_{2\phi,T}$. The transition criteria can be visualised in a $G - x$ map, where G_T is obtained from $Re_{2\phi} = Re_{2\phi,T}$, i.e.

$$\frac{Gx}{\mu_V} + \frac{G(1-x)D}{\mu_L} = 10^8 \; D^{1.5} \tag{21}$$

obtaining G_T at the transition as

$$G_T = \frac{10^8 \; D^{1/2}}{x/\mu_V + (1-x)/\mu_L} \tag{22}$$

The effect of the pipe diameter on G_T for R134a at $T_s = 40°C$ is shown in figure (12). Reducing the diameter of the pipe, the transition occurs at lower qualities and lower mass fluxes. In particular, it is possible to see that as the pipe diameter is reduced Nu_I becomes the dominant contribution to the heat transfer coefficient.

2.4. Evaluation of previous correlations

The models from Cavallini et al [21] and from Shah [18] are evaluated against the experimental data base used in this work and shown in Figure (13) and (14) respectively. The plots are showing the error in terms of Nu_{cal}/Nu_{exp} versus the thermodynamic quality. The model from Cavallini et al. for the ΔT-independent regime, i.e. $J_G > J_G^T$ Eq.8, shows good agreement with the experimental data points predicting 78.7% of data points to within ±30% but including 9 adjusting parameters in the model. Similarly, the model from Shah (2009) for $J_G > J_G^T$ shows good agreement with the experimental data points predicting 65.6% of data points to within ±30% with a model considering 11 adjusting parameters. As it is possible to see, both models show good prediction capabilities although these two models considers different dimensionless groups. Analysing the hydrodynamic component of both models, it is possible to see that it can be considered as an alternative expression of $Re_{2\phi}$ as shown in Figure (15) and (16). In particular, it is noticed that the case corresponding to water shows a major deviation for these two models which also result in a large error. Unfortunately, experiments of flow condensation using water as working fluid are scarce.

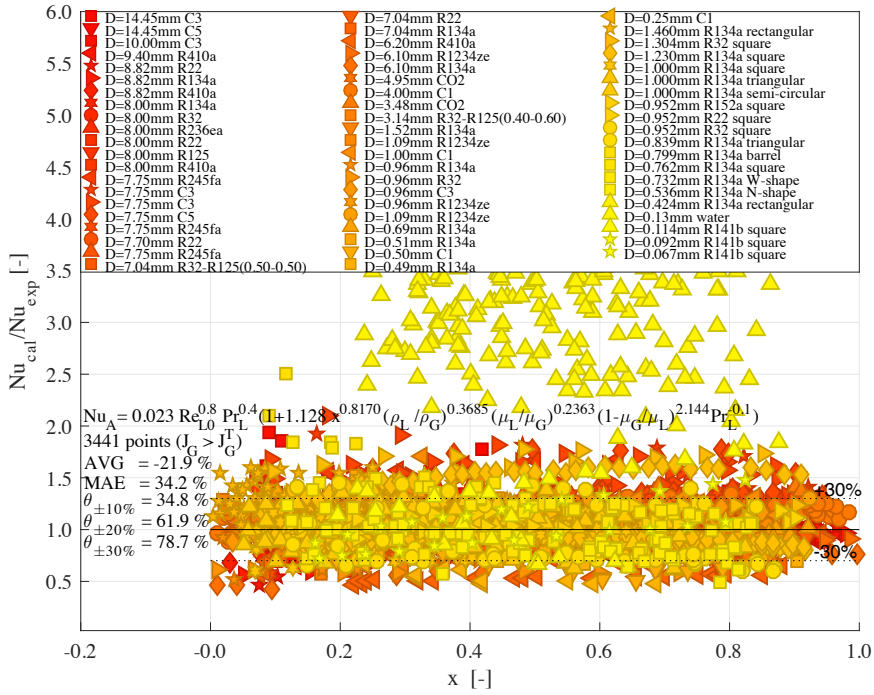

Figure 13: Evaluation of the model from Cavallini[21] in terms of the thermodynamic quality.

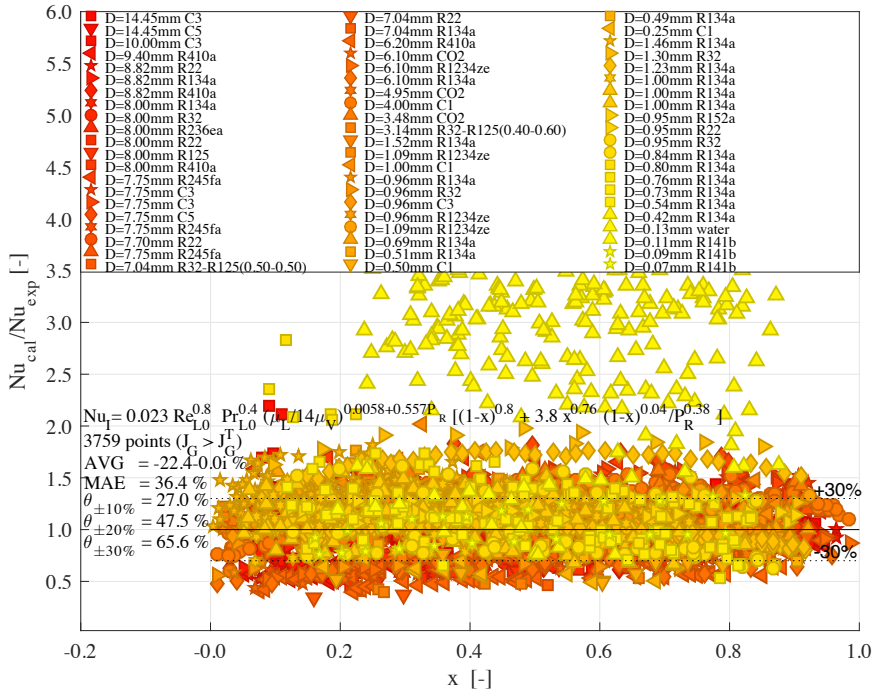

Figure 14: Evaluation of the model from Shah (2009) [18] in terms of the thermodynamic quality.

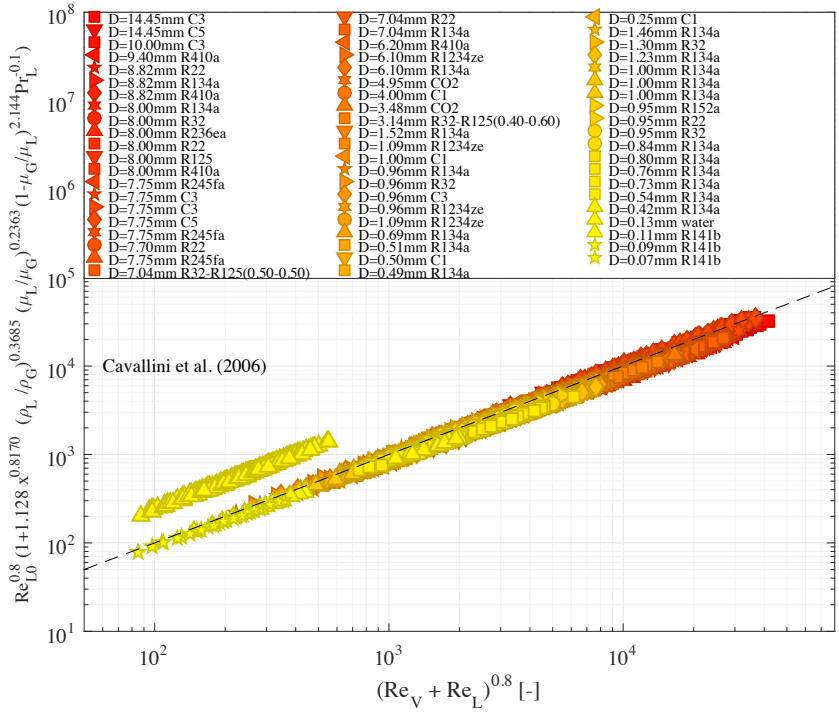

Figure 15: Analysis of the model from Cavallini[21] in terms of $Re_{2\phi}$.

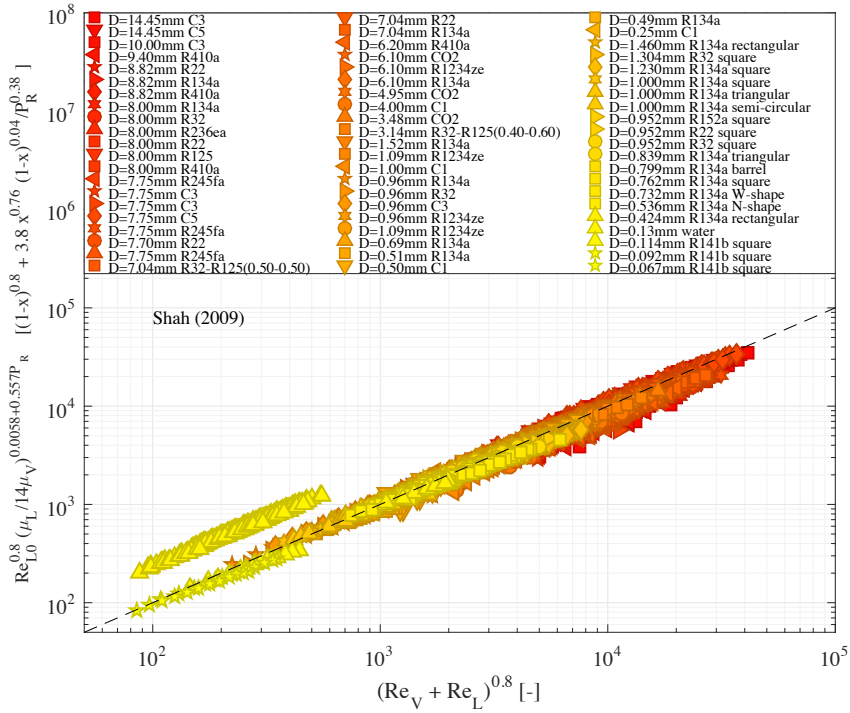

Figure 16: Analysis of the model from Shah [18] in terms of $Re_{2\phi}$.

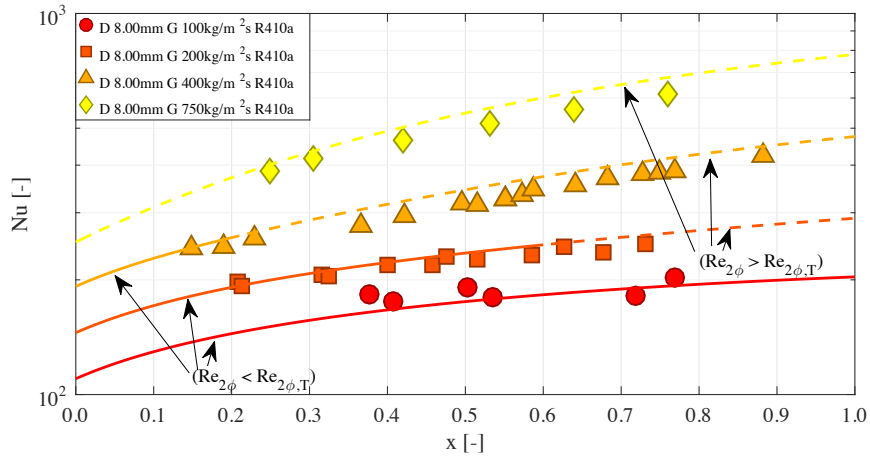

Figure 17: Prediction of the heat transfer coefficient by the present model during the condensation of R410a inside a 8 mm diameter pipe [21].

2.5. Prediction of heat transfer coefficients

A comparison between some selected experimental data points and the new model are discussed in this section. Figure (17) and (18) show the case of two different pipe diameters corresponding to 0.96 *mm* [44] and 8 *mm* [21] respectively. The calculated heat transfer coefficient is shown as a continuous dash line for region I and a continuous line for region II in figure (17). The new model is able to predict quantitatively the data from low to high qualities. Unfortunately, there are scarce experimental data available on the region close to 0 quality including data points in the all liquid region for further evaluating the model. It is expected that the model related to region II (continuous line) should show a transition to the Dittus-Boelter correlation as the quality approaches 0. In figure (18), the model from Cavallini et al. (2006) is also shown which is also able to predict the experimental data set. On the other hand, figure (19) shows a comparison with experimental data corresponding to water [53]. In this case, it is possible to see that the model from Cavallini et al. (2006) shows a large deviation. Finally, figure (20) shows examples corresponding to the prediction of hydrocarbons in pipe diameters of 14.45, 7.75 and 1.00 mm for pentane and propane [27] and for methane [43].

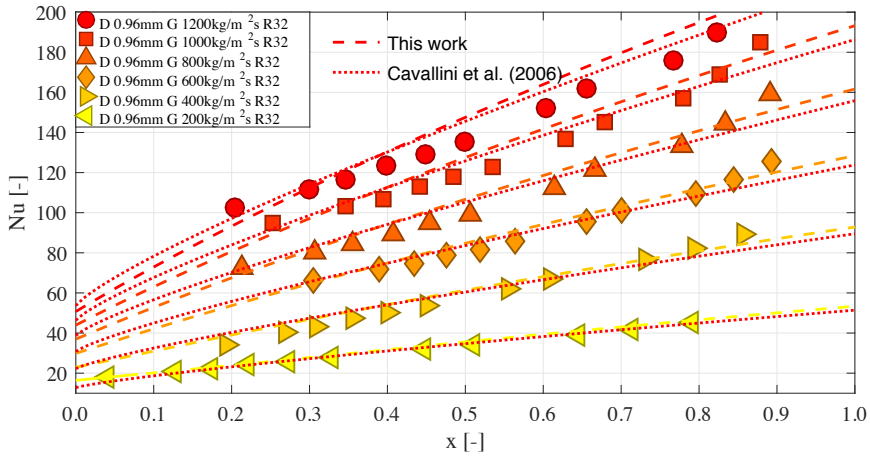

Figure 18: Prediction of the heat transfer coefficient by the present model and the one from Cavalli et al. (2006) during the condensation of R32 inside a 0.96 mm diameter pipe [44].

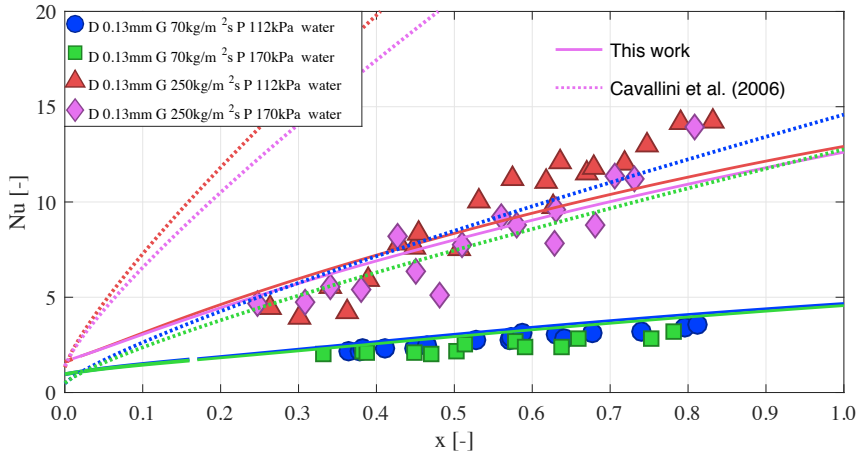

Figure 19: Prediction of the heat transfer coefficient by the present model during the condensation of water in a microchannel [53].

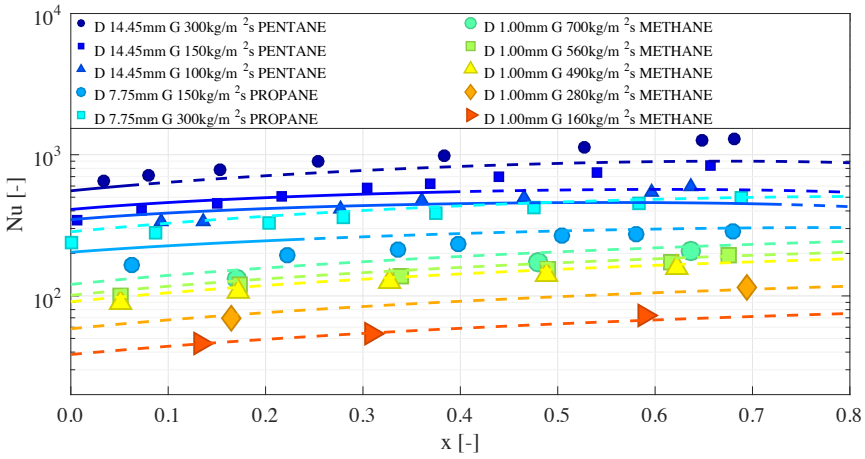

Figure 20: Prediction of the heat transfer coefficient by the present model during the condensation of pentane, propane [27] and methane [43].

3. Conclusions

In this work, a simple and general model to determine the flow condensation heat transfer coefficient inside plain pipes is presented. The model considers two regimes corresponding to high mass fluxes and/or high thermodynamic qualities and low mass fluxes and/or low thermodynamic qualities. For each region, a model is suggested which resembles the single-phase heat transfer coefficient model but defining an equivalent Reynolds number in terms of the sum of the superficial liquid and vapour Reynolds numbers. The models consider that the superficial vapour Reynolds number play a major role in controlling the heat transfer coefficient. The similitude of the proposed model to the single phase heat transfer coefficient model might indicate that similar heat transfer mechanisms are dominant in both situations. This fact might imply that a derived model for the single phase heat transfer coefficient can be applicable for predicting the flow condensation heat transfer coefficient if the definition of the Reynolds and Prandtl number are replaced for equivalent two phase numbers suggested in this work. The model is able to predict the heat transfer coefficient from channels with a hydraulic diameter of 67 μm up to pipes with a hydraulic diameter of 20 mm for several fluids. No noticeable effect of the diameter of the channel, shape or fluid properties on the heat transfer coefficient has been observed for the studied cases.

4. Acknowledgements

Funding for this work from the Research Council of Norway under the FRINATEK project 231529 is gratefully acknowledged.

5. References

[1] J. C. Pacio, C. A. Dorao, A review on heat exchanger thermal hydraulic models for cryogenic applications, Cryogenics 51 (7) (2011) 366–379. doi:10.1016/j.cryogenics.2011.04.005.
URL http://dx.doi.org/10.1016/j.cryogenics.2011.04.005

[2] A. Cavallini, G. Censi, D. Del Col, L. Doretti, G. A. Longo, L. Rossetto, C. Zilio, Condensation inside and outside smooth and enhanced tubes -a review of recent research, International Journal of Refrigeration 26 (4) (2003) 373–392. doi:10.1016/S0140-7007(02)00150-0.

[3] S. M. Kim, I. Mudawar, Universal approach to predicting heat transfer coefficient for condensing mini/micro-channel flow, International Journal of Heat and Mass Transfer 56 (1-2) (2013) 238–250. doi:10.1016/j.ijheatmasstransfer.2012.09.032.
URL http://dx.doi.org/10.1016/j.ijheatmasstransfer.2012.09.032

[4] V. G. Rifert, V. V. Sereda, Condensation inside smooth horizontal tubes: Part 1. Survey of the methods of heat-exchange prediction, Thermal Science 19 (5) (2015) 1769–1789. doi:10.2298/TSCI140522036R.

[5] S. Garimella, B. M. Fronk, Encyclopedia of two-phase heat transfer and flow I: Condensation heat transfer, 2016.

[6] R. H. S. Winterton, Where did the Dittus and Boelter equation come from?, Int. J. Heat Mass Transfer 41 (4-5) (1998) 809–810. doi:10.1016/j.rmr.2010.03.023.

[7] F. W. Dittus, L. M. K. Boelter, Heat transfer in automobile radiators of the tubular type, International Communications in Heat and Mass Transfer 12 (1) (1985) 3–22. doi:10.1016/0735-1933(85)90003-X.

[8] B. Petukhov, Heat Transfer and Friction in Turbulent Pipe Flow with Variable Physical Properties, Advances in Heat Transfer 6 (1970) 503–564. doi:10.1016/S0065-2717(08)70153-9.
URL http://www.sciencedirect.com/science/article/pii/S0065271708701539

[9] C. A. Sleicher, M. W. Rouse, A convenient correlation for heat transfer to constant and variable property fluids in turbulent pipe flow, International Journal of Heat and Mass Transfer 18 (5) (1975) 677–683. doi:10.1016/0017-9310(75)90279-3.

[10] V. Gnielinski, Heat transfer coefficients for turbulent flow in concentric annular ducts, Heat Transfer Engineering 30 (6) (2009) 431–436. doi:10.1080/01457630802528661.

[11] O. K. Crosser, Condensing heat transfer within horizontal tubes, Ph.D. thesis, Rice University (1955).

[12] H. F. Rosson, Heat transfer during condensation inside a horizontal tube, Ph.D. thesis, Rice University. (1957).

[13] E. N. Sieder, G. E. Tate, Heat Transfer and Pressure Drop of Liquids in Tubes, Industrial and Engineering Chemistry 28 (1936) 1429–1435. doi:10.1021/ie50324a027.

[14] J. Goodykoontz, R. Dorsch, Local heat-transfer coefficients for condensation of steam in vertical downflow within a 5/8-inch-diameter Tube, Tech. Rep. March (1966).

[15] J. Goodykoontz, R. Dorsch, Local Heat-Transfer Coefficients and Static Pressures for Condensation of High-Velocity Steam Within a Tube, Tech. Rep. May (1967).

[16] R. Cavallini, A., & Zecchin, A dimensionless correlation for heat transfer in forced convection condensation, Sixth International Heat Transfer Conference Tokyo (2) (1974) 309–313.

[17] M. M. Shah, A general correlation for heat transfer during film condensation inside pipes, International Journal of Heat and Mass Transfer 22 (4) (1979) 547–556. doi:10.1016/0017-9310(79)90058-9.

[18] M. M. Shah, An Improved and Extended General Correlation for Heat Transfer During Condensation in Plain Tubes, HVAC&R Research 15 (5) (2009) 889–914.

[19] T. N. Tandon, H. K. Varma, C. P. Gupta, Heat transfer during forced convection condensation inside horizontal tube, International Journal of Refrigeration 18 (3) (1995) 210–214. doi:10.1016/0140-7007(95)90316-R.

[20] M. K. Dobson, J. C. Chato, Condensation in Smooth Horizontal Tubes, Journal of Heat Transfer 120 (1) (1998) 193–213. doi:10.1115/1.2830043. URL http://dx.doi.org/10.1115/1.2830043

[21] A. Cavallini, D. D. Col, L. Doretti, M. Matkovic, L. Rossetto, C. Zilio, G. Censi, Condensation in Horizontal Smooth Tubes: A New Heat Transfer Model for Heat Exchanger Design, Heat Transfer Engineering 27 (8) (2006) 31–38. doi:10.1080/01457630600793970. URL http://www.tandfonline.com/doi/abs/10.1080/01457630600793970

[22] C. A. Dorao, M. Fernandino, Dominant dimensionless groups controlling heat transfer coefficient during flow condensation inside pipes, Journal of Heat and Mass Transfer (2017) in press.

[23] H. Groothuis, W. Hendal, Heat transfer in two-phase flow, Chemical Engineering Science 11 (1959) 212–220.

[24] G. Elamvaluthi, N. S. Srinivas, Two-phase heat transfer in two component vertical flows, International Journal of Multiphase Flow 10 (2) (1984) 237–242. doi:10.1016/0301-9322(84)90021-1.

[25] E. W. Lemmon, M. L. Huber, M. O. McLinden, NISTReference Fluid Thermodynamic and Transport Properties-REFPROP, Tech. rep. (2013).

[26] C. Aprea, A. Greco, G. P. Vanoli, Condensation heat transfer coefficients for R22 and R407C in gravity driven flow regime within a smooth horizontal tube, International Journal of Refrigeration 26 (4) (2003) 393–401. doi:10.1016/S0140-7007(02)00151-2.

[27] M. Macdonald, Condensation of pure and zeotropic hydrocarbons in smooth horizontal tubes, Ph.D. thesis, Georgia Institute of Technology (2015).

[28] J. A. Milkie, Condensation of hydrocarbons and zeotropic hydrocarbon/refrigerant mixtures in horizontal tubes, Phd thesis, Georgia Institute of Technology (2014).

[29] J. Yu, J. Chen, F. Li, W. Cai, L. Lu, Y. Jiang, Experimental investigation of forced convective condensation heat transfer of hydrocarbon refrigerant in a helical tube, Applied Thermal Engineering in press. doi:10.1016/j.applthermaleng.2017.10.143.
URL https://doi.org/10.1016/j.applthermaleng.2017.10.143

[30] B. Mitra, Supercritical gas cooling and condensation of refrigerant R410A at near-critical pressures, Ph.D. thesis, Georgia Institute of Technology (2005).

[31] D. Jung, Y. Cho, K. Park, Flow condensation heat transfer coefficients of R22, R134a, R407C, and R410A inside plain and microfin tubes, International Journal of Refrigeration 27 (1) (2004) 25–32. doi:10.1016/S0140-7007(03)00122-1.

[32] A. Cavallini, G. Censi, D. Del Col, L. Doretti, G. A. Longo, L. Rossetto, Experimental investigation on condensation heat transfer and pressure

drop of new HFC refrigerants (R134a, R125, R32, R410A, R236ea) in a horizontal smooth tube, International Journal of Refrigeration 24 (1) (2001) 73–87. doi:10.1016/S0140-7007(00)00070-0.

[33] G. Ghim, J. Lee, Condensation heat transfer of low GWP ORC working fluids in a horizontal smooth tube, International Journal of Heat and Mass Transfer 104 (2017) 718–728. doi:10.1016/j.ijheatmasstransfer.2016.08.090.
URL http://linkinghub.elsevier.com/retrieve/pii/S0017931016306329

[34] J. Y. Shin, M. S. Kim, S. T. Ro, Experimental study on forced convective boiling heat transfer of pure refrigerants and refrigerant mixtures in a horizontal tube, International Journal of Refrigeration 20 (4) (1997) 267–275. doi:10.1016/S0140-7007(97)00004-2.

[35] C. Kondou, P. Hrnjak, Heat rejection from R744 flow under uniform temperature cooling in a horizontal smooth tube around the critical point coulement du R744 a ‘ l ’ inte rieur d ’ un Rejet de chaleur lors de l ’ e tube lisse horizontal sous des conditions de refroidisseme, International Journal of Refrigeration 34 (3) (2011) 719–731. doi:10.1016/j.ijrefrig.2010.11.003.
URL http://dx.doi.org/10.1016/j.ijrefrig.2010.11.003

[36] R. Agarwal, P. Hrnjak, ScienceDirect Condensation in two phase and desuperheating zone for R1234ze (E), R134a and R32 in horizontal smooth tubes surchauffe Condensation dans la zone diphasique et de d e pour le R1234ze (E), le R134a et le R32 dans des tubes lisses horizonta, International Journal of Refrigeration 50 (1991) (2015) 172–183. doi:10.1016/j.ijrefrig.2014.10.015.
URL http://dx.doi.org/10.1016/j.ijrefrig.2014.10.015

[37] J. Xiao, P. Hrnjak, Heat transfer and pressure drop of condensation from superheated vapor to subcooled liquid, International Journal of Heat and Mass Transfer 103 (2016) 1327–1334. doi:10.1016/j.ijheatmasstransfer.2016.08.036.
URL http://dx.doi.org/10.1016/j.ijheatmasstransfer.2016.08.036

[38] C. H. Son, H. K. Oh, Condensation heat transfer characteristics of CO 2 in a horizontal smooth- and microfin-tube at high saturation temperatures, Applied Thermal Engineering 36 (1) (2012) 51–62.

doi:10.1016/j.applthermaleng.2011.12.017.
URL http://dx.doi.org/10.1016/j.applthermaleng.2011.12.017

[39] J. Xiao, P. Hrnjak, A heat transfer model for condensation accounting for non-equilibrium effects, International Journal of Heat and Mass Transfer 111 (2017) 201–210. doi:10.1016/j.ijheatmasstransfer.2017.03.019.
URL http://dx.doi.org/10.1016/j.ijheatmasstransfer.2017.03.019

[40] Y. J. Kim, J. Jang, P. S. Hrnjak, M. S. Kim, Condensation Heat Transfer of Carbon Dioxide Inside Horizontal Smooth and Microfin Tubes at Low Temperatures, Journal of Heat Transfer 130 (November) (2008) 111001. doi:10.1115/1.2957595.
URL http://dx.doi.org/10.1115/1.2957595%5Cnhttp://heattransfer.asmedigitalc

[41] T. M. Bandhauer, A. Agarwal, S. Garimella, Measurement and modeling of condensation heat transfer coefficients in circular microchannels, Journal of Heat Transfer 128 (October) (2006) 1050–1059. doi:10.1088/0960-1317/18/8/085012.
URL http://dx.doi.org/10.1115/1.2345427

[42] N. Liu, H. Xiao, J. Li, Experimental investigation of condensation heat transfer and pressure drop of propane, R1234ze(E) and R22 in minichannels, Applied Thermal Engineering 102 (2016) 63–72. doi:10.1016/j.applthermaleng.2016.03.073.
URL http://dx.doi.org/10.1016/j.applthermaleng.2016.03.073

[43] K. A. Maråk, Knut Arild Maråk Condensation Heat Transfer and Pressure Drop for Methane and Binary Methane Fluids in Small Channels, Ph.D. thesis, Norwegian University of Science and Technology (2009).

[44] M. Matkovic, A. Cavallini, D. Del Col, L. Rossetto, Experimental study on condensation heat transfer inside a single circular minichannel, International Journal of Heat and Mass Transfer 52 (9-10) (2009) 2311–2323. doi:10.1016/j.ijheatmasstransfer.2008.11.013.
URL http://dx.doi.org/10.1016/j.ijheatmasstransfer.2008.11.013

[45] D. Del Col, S. Bortolin, M. Bortolato, L. Rossetto, Condensation heat transfer and pressure drop with propane in a minichannel, International refrigeration and air conditioning conference at Purdue 1. arXiv:arXiv:1011.1669v3, doi:10.1017/CBO9781107415324.004.

[46] D. Del Col, M. Azzolin, S. Bortolin, C. Zilio, D. Del, M. Azzolin, S. Bortolin, C. Zilio, D. D. E. L. Col, M. Azzolin, S. Bortolin, C. Zilio, Two-phase pressure drop and condensation heat transfer of R32 / R1234ze (E) non-azeotropic mixtures inside a single microchannel, Science and Technology for the Built Environment 21 (5) (2015) 595–605. doi:10.1080/23744731.2015.1047718.

[47] J. S. Shin, M. H. Kim, An Experimental Study of Flow Condensation Heat Transfer Inside Circular and Rectangular Mini-Channels, Heat Transfer Engineering 26 (3) (2005) 36–44. doi:10.1080/01457630590907185.

[48] W. W. W. Wang, T. D. Radcliff, R. N. Christensen, A condensation heat transfer correlation for millimeter-scale tubing with flow regime transition, Experimental Thermal and Fluid Science 26 (5) (2002) 473–485. doi:10.1016/S0894-1777(02)00162-0.

[49] N. Liu, J. Li, Experimental study on condensation heat transfer of R32, R152a and R22 in horizontal minichannels, Applied Thermal Engineering 90 (2015) 763–773. doi:10.1016/j.applthermaleng.2015.07.062.
URL http://dx.doi.org/10.1016/j.applthermaleng.2015.07.062

[50] D. Del Col, S. Bortolin, A. Cavallini, M. Matkovic, Effect of cross sectional shape during condensation in a single square minichannel, International Journal of Heat and Mass Transfer 54 (17-18) (2011) 3909–3920. doi:10.1016/j.ijheatmasstransfer.2011.04.035.
URL http://dx.doi.org/10.1016/j.ijheatmasstransfer.2011.04.035

[51] M. Derby, H. Joon, Y. Peles, M. K. Jensen, International Journal of Heat and Mass Transfer Condensation heat transfer in square, triangular, and semi-circular mini-channels, International Journal of Heat and Mass Transfer 55 (1-3) (2012) 187–197. doi:10.1016/j.ijheatmasstransfer.2011.09.002.
URL http://dx.doi.org/10.1016/j.ijheatmasstransfer.2011.09.002

[52] A. Agarwal, T. M. Bandhauer, S. Garimella, Measurement and modeling of condensation heat transfer in non-circular microchannels ‘ l ’ inte rieur des Transfert de chaleur lors de la condensation a lisation microcanaux non circulaires : mesures et mode, International Journal of Re-

frigeration 33 (6) (2010) 1169–1179. doi:10.1016/j.ijrefrig.2009.12.033. URL http://dx.doi.org/10.1016/j.ijrefrig.2009.12.033

[53] Z. Zhang, Y. Peles, M. K. Jensen, Condensation Heat Transfer in Ultracompact Minichannel Heat Exchangers, Journal of Thermal Science and Engineering Applications 6 (1) (2013) 011003. doi:10.1115/1.4024902. URL http://thermalscienceapplication.asmedigitalcollection.asme.org/article

[54] T. Dong, Z. Yang, Measurement and modeling of R141b condensation heat transfer in silicon rectangular microchannels, Journal Micromechanics and Microengineering 18 (2008) 085012. doi:10.1088/0960-1317/18/8/085012.

[55] M. Hishida, Y. Nagano, S. Teruhumi, Structure of Turbulent Velocity and Temperature Fluctuations in Fully Developed Pipe Flow, Transactions of the Japan Society of Mechanical Engineers 44 (February 1979) (1978) 126–134. doi:10.1299/kikai1938.44.126.

[56] H. Kawamura, K. Ohsaka, H. Abe, K. Yamamoto, DNS of turbulent heat transfer in channel flow with low to medium-high Prandtl number fluid, International Journal of Heat and Fluid Flow 19 (5) (1998) 482–491. doi:10.1016/S0142-727X(98)10026-7.

[57] L. Redjem-Saad, M. Ould-Rouiss, G. Lauriat, Direct numerical simulation of turbulent heat transfer in pipe flows: Effect of Prandtl number, International Journal of Heat and Fluid Flow 28 (5) (2007) 847–861. doi:10.1016/j.ijheatfluidflow.2007.02.003.

[58] C. A. Dorao, O. B. Fernandez, M. Fernandino, Experimental study of horizontal flow boiling heat transfer of R134a at a saturation temperature of 18.6○ C, Journal of Heat Transfer 139 (2017) 111510.

[59] P. S. Lee, S. V. Garimella, D. Liu, Investigation of heat transfer in rectangular microchannels, International Journal of Heat and Mass Transfer 48 (9) (2005) 1688–1704. doi:10.1016/j.ijheatmasstransfer.2004.11.019.

[60] A. Diani, A. Cavallini, L. Rossetto, R1234yf condensation inside a 3.4 mm ID horizontal microfin tube Condensation de, International Journal of Refrigeration 75 (2017) 178–189. doi:10.1016/j.ijrefrig.2016.12.014. URL http://dx.doi.org/10.1016/j.ijrefrig.2016.12.014

[61] J.-P. Bukasa, L. Liebenberg, J. P. Meyer, Condensation Inside Spiralled Micro-Fin Tubes, Journal of Heat Transfer 126 (June) (2004) 321–328. doi:10.1115/1.1737777.

[62] G.-q. Li, Z. Wu, W. Li, Z.-k. Wang, X. Wang, H.-x. Li, S.-c. Yao, Experimental investigation of condensation in micro-fin tubes of different geometries, Experimental Thermal and Fluid Science 37 (2012) 19–28. doi:10.1016/j.expthermflusci.2011.09.008.
URL http://dx.doi.org/10.1016/j.expthermflusci.2011.09.008

[63] S. W. Churchill, R. Usagi, A general expression for the correlation of rates of transfer and other phenomena, AIChE Journal 18 (6) (1972) 1121–1128. doi:10.1002/aic.690180606.